

Geophysical Research Letters[®]



RESEARCH LETTER

10.1029/2023GL104158

Surface-Forced Variability in the Nordic Seas Overturning Circulation and Overflows

Marius Årthun¹ 

¹Geophysical Institute, University of Bergen, and Bjerknes Centre for Climate Research, Bergen, Norway

Key Points:

- Variable transport of Nordic overflow waters is determined by surface forcing in the Norwegian Sea
- Nordic Seas overturning circulation shows pronounced multidecadal variability since 1950
- The overturning circulation and overflow are projected to decrease toward 2040

Supporting Information:

Supporting Information may be found in the online version of this article.

Correspondence to:

M. Årthun,
marius.arthun@uib.no

Citation:

Årthun, M. (2023). Surface-forced variability in the Nordic Seas overturning circulation and overflows. *Geophysical Research Letters*, 50, e2023GL104158. <https://doi.org/10.1029/2023GL104158>

Received 19 APR 2023

Accepted 5 JUL 2023

Abstract Water mass transformation in the Nordic Seas and the associated overflow of dense waters across the Greenland-Scotland Ridge (GSR) acts to maintain the lower limb of the Atlantic meridional overturning circulation. Here, we use ocean and atmospheric reanalysis to assess the temporal variability in the Nordic Seas overturning circulation between 1950 and 2020 and its relation to surface buoyancy forcing. We find that variable surface-forced transformation of Atlantic waters in the eastern Nordic Seas can explain variations in overflow transport across the GSR. The production of dense water masses in the Greenland and Iceland Seas is of minor importance to overflow variability. The Nordic Seas overturning circulation shows pronounced multidecadal variability that is in phase with the Atlantic Multidecadal Variability (AMV) index, but no long-term trend. As the AMV is currently transitioning into its negative phase, the next decades could see a decreased overflow from the Nordic Seas.

Plain Language Summary In the Nordic Seas, warm, light waters are transformed into cold, dense waters. This dense-water formation is important to the global ocean circulation. In this study, we quantify the role of surface heat and freshwater fluxes in this dense-water formation. We find that variable surface fluxes in the eastern Nordic Seas can largely explain variations in dense-water formation since 1950. The formation of dense waters in the Nordic Seas and the subsequent export of these waters into the North Atlantic show no long-term trend. We nevertheless predict that the dense-water formation will decrease during the next decade as a result of multidecadal variability.

1. Introduction

In the Nordic Seas, warm waters of Gulf Stream origin releases its heat to the atmosphere and returns south to the North Atlantic as a cold, dense current at depth (Brakstad et al., 2023; Chafik & Rossby, 2019; Eldevik & Nilsen, 2013; Smedsrud et al., 2022) (Figure 1a). This dense overflow water feeds the lower limb of the Atlantic Meridional Overturning Circulation (AMOC) (Dickson & Brown, 1994; Swift et al., 1980) and is therefore an important component of the global ocean circulation. The North Atlantic and Nordic Seas are separated by the Greenland-Scotland Ridge (GSR) and the main exchange of water masses takes place through the Denmark Strait (DS), the Iceland-Faroe Ridge, and the Faroe-Shetland Channel (FSC) (Hansen & Østerhus, 2000; Østerhus et al., 2019).

The overflows across the GSR are composed of two distinct types of overflow water: an “Atlantic-origin” overflow water that is formed by ocean heat loss to the atmosphere along the cyclonic boundary current system of the Nordic Seas (Eldevik et al., 2009; Mauritzen, 1996), and an “Arctic-origin” overflow water that is produced by open-ocean convection in the interior basins of the western Nordic Seas (Huang et al., 2020; Swift & Aagaard, 1981). The volume transport associated with the two components of overflow water is comparable (Hansen & Østerhus, 2000; Våge et al., 2011). However, it is not established whether the two types of overflow water contributes equally to *changes* in overflow transport on interannual to decadal time scales.

Common for both Atlantic-origin and Arctic-origin overflow water is the importance of surface buoyancy forcing. Using observed hydrography and an inverse model of oceanic transports, Isachsen et al. (2007) identified a close correspondence between the surface transformation in the Nordic Seas and the average strength of the overturning circulation. Similarly, a clear link has been found between surface-forced water mass transformation and the North Atlantic overturning circulation (Desbruyères et al., 2019; Marsh, 2000; Megann et al., 2021). However, temporal variability in the Nordic Seas overturning circulation and its relation to surface forcing has not yet been assessed. In this study, we accordingly use observations, and ocean and atmospheric reanalysis to investigate the Nordic Seas overturning circulation in recent decades (1950–2020). We will in particular assess to what extent

© 2023. The Authors.

This is an open access article under the terms of the [Creative Commons Attribution License](https://creativecommons.org/licenses/by/4.0/), which permits use, distribution and reproduction in any medium, provided the original work is properly cited.

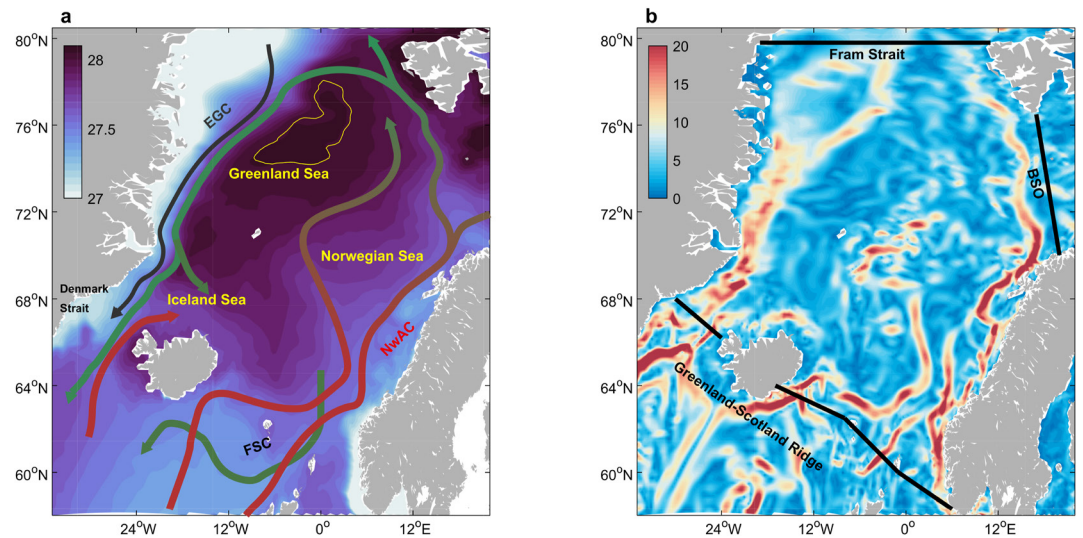


Figure 1. (a) Map showing the main ocean currents into and out of the Nordic Seas. Red arrows indicate warm surface waters, while green arrows indicate cold dense waters that eventually leave the Nordic Seas as overflow waters predominantly through the Faroe Shetland Channel and Denmark Strait. The blue arrow shows the cold, fresh East Greenland Current. The background color shows the mean surface density (σ_θ ; kg m⁻³) in March 2009–2018. The yellow contour shows where the mixed-layer depth in March exceeds 1,500 m. NwAC: Norwegian Atlantic Current. (b) Surface current speed (cm s⁻¹) in March 2018. The black lines show the boundaries of the Nordic Seas as used in this study. BSO, Barents Sea Opening.

variable surface-forced water mass transformation by heat and freshwater fluxes can explain variations in overflow transport across the GSR. This will improve our understanding of how the Nordic Seas overflows respond to changes in surface forcing, which is important in order to predict potential future changes in a warming climate.

2. Data and Methods

2.1. Observations of Overflow Transports

Transports of overflow water ($\sigma_\theta > 27.80$ kg m⁻³) across the GSR is provided by the AtlantOS consortium (OceanSITES, 2022). We consider data from the Faroe Bank Channel (Hansen et al., 2016) and the DS (Jochumsen et al., 2017). The combined time series covers the period 1997 to 2015. Holes in the time series were filled by linear interpolation.

2.2. ORAS5

To investigate circulation changes in the Nordic Seas we use the global ocean and sea ice reanalysis ORAS5 (Ocean Reanalysis System 5; Zuo et al., 2019) covering the time period 1979–2018. The ORAS5 system uses the Nucleus for European Modeling of the Ocean (NEMO) ocean model, the LIM2 sea ice model, and the NEMOVAR ocean assimilation system. The horizontal resolution is $1/4^\circ \times 1/4^\circ$ (approximately 12 km in the Nordic Seas) and there are 75 vertical levels (level spacing increasing from 1 m at the surface to 200 m in the deep ocean). The atmospheric forcing of ORAS5 is from ERA-40 (before 1979), ERA-Interim (1979–2015), and ECMWF NWP (2015–present). ORAS5 consists of five ensemble members generated by the perturbation of initial conditions, observations and forcings. Here we mainly use the first unperturbed member. In addition, we make use of the ORAS5 backward extension (ORAS5-BE) covering the period 1958–1978 with one ensemble member (Zuo et al., 2019).

ORAS5 has previously been evaluated for the Nordic Seas and Arctic Ocean and shown to perform well (Carton et al., 2019; Li et al., 2022; Shu et al., 2021). The horizontal resolution is sufficient to adequately resolve the different branches of Atlantic water (Orvik & Niiler, 2002) and the southward flow east of Greenland (Figure 1b). Consistent with observations (e.g., Eldevik & Nilsen, 2013), three distinct water masses are present at the GSR (Figure 2a; vertical profiles shown in Figure S1 of Supporting Information S1); warm and saline Atlantic Water

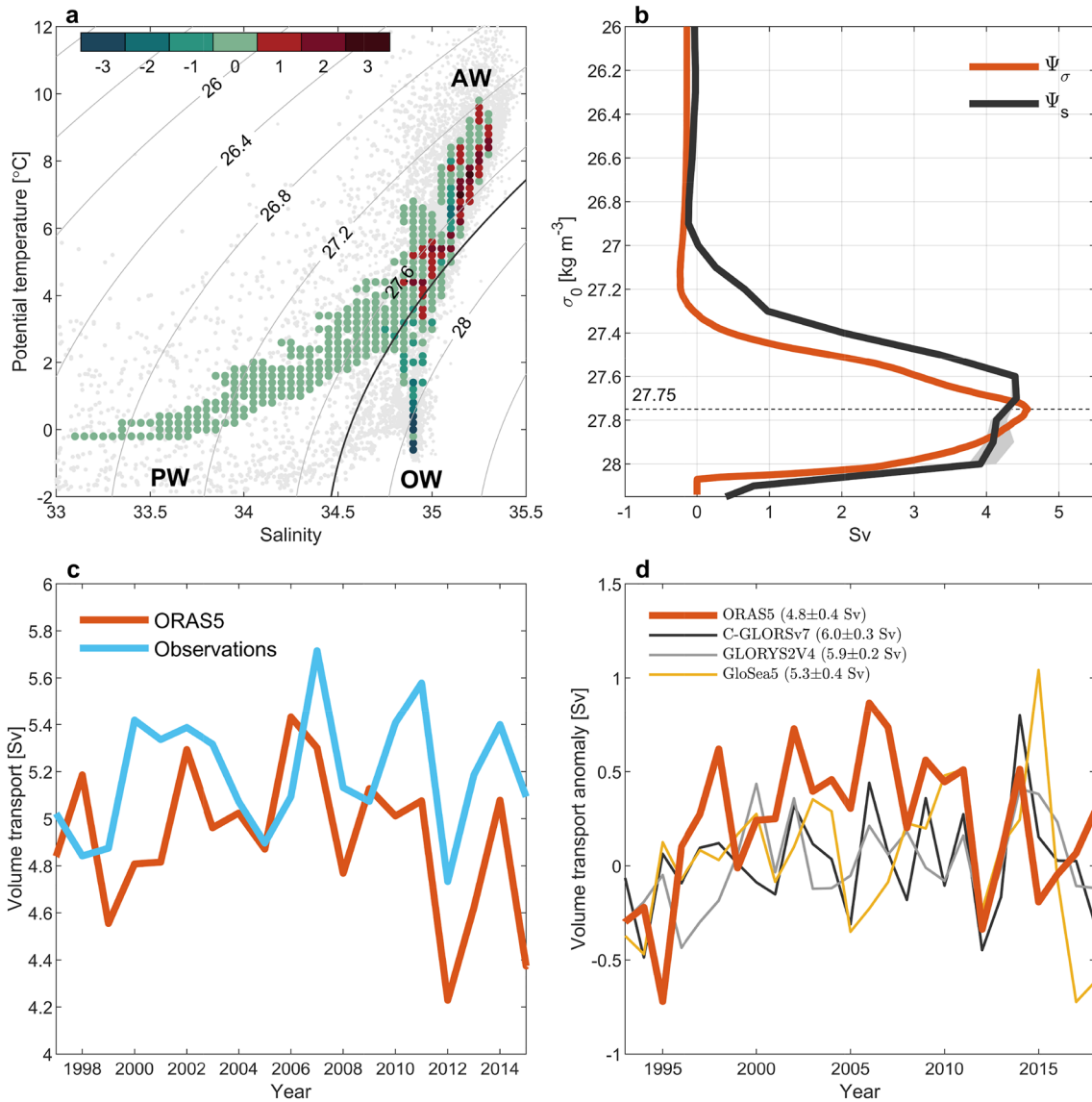


Figure 2. (a) Observed (gray dots) and simulated (ORAS5; colored dots) temperature-salinity (TS) characteristics of waters at the Greenland-Scotland Ridge (GSR). The color corresponds to volume transport (in 10^{-1} Sv) per TS-class (bin size of 0.2°C and 0.05 g kg^{-1}). Positive transports are into the Nordic Seas. The observations are from Eldevik and Nilsen (2013). (b) Time series of overflow transport from observations and ORAS5 between 1997 and 2015. (c) Mean streamfunctions of the density-space overturning at the GSR (Ψ_σ) and of the surface-forced overturning in the Nordic Seas (Ψ_s) between 1979 and 2018 from ORAS5. The gray shading is the ORAS5 ensemble spread for Ψ_s . (d) Overflow transport anomalies between 1993 and 2018 in four ocean reanalyses. Mean value and standard deviation for each reanalysis are provided.

(AW; $\theta > 4^\circ\text{C}$, $\sigma_\theta < 27.75 \text{ kg m}^{-3}$), cold and fresh Polar Water (PW; $\theta < 4^\circ\text{C}$, $\sigma_\theta < 27.75 \text{ kg m}^{-3}$), and cold, dense Overflow Water (OW; $\sigma_\theta > 27.75 \text{ kg m}^{-3}$). Note that OW in ORAS5 is defined by $\sigma_\theta > 27.75 \text{ kg m}^{-3}$ whereas observations use $\sigma_\theta > 27.8 \text{ kg m}^{-3}$. This is based on the overturning streamfunction, which for ORAS5 reaches its maximum at 27.75 kg m^{-3} (Figure 2b). For the time period when observations of volume transport across the GSR exist (1997–2015), the mean transport of these water masses consists of a net AW inflow of 6.1 Sv ($1 \text{ Sv} \equiv 10^6 \text{ m}^3 \text{ s}^{-1}$), and an outflow of 4.9 Sv of OW (2.5 and 2.4 Sv east and west of Iceland, respectively) and 1.2 Sv of PW. These values are in broad agreement with available observations (Østerhus et al., 2019). Inter-annual variability in OW transport from ORAS5 is also similar to observations (Figure 2c; $r = 0.53$, $p = 0.01$) and to that in three other commonly used ocean reanalyses (Figure 2d); C-GLORSv7 (Storto & Masina, 2016), GLORYS2V4 (Ferry et al., 2012), and GloSea5 (MacLachlan et al., 2015). In agreement with observations (Brakstad et al., 2019), deep mixed-layers, reflecting open-ocean convection, are found in the Greenland Sea (Figure 1a).

2.3. Surface-Forced Overturning Circulation

The meridional overturning circulation involves the transformation of warm northward-flowing surface waters into cold, dense waters flowing southwards at depth. The AMOC is thus directly associated with water mass transformation, and previous studies have shown that the density-space overturning circulation can be well represented by water mass transformations from surface buoyancy fluxes (e.g., Desbruyères et al., 2019; Marsh, 2000; Petit et al., 2020). The calculation of the surface-forced component of the overturning circulation detailed below follows these studies.

The surface-forced overturning streamfunction relates the rate of density transformation in a given density class to the surface buoyancy fluxes into that density class over its outcrop area, neglecting the effects of subsurface mixing and local changes in storage (Speer & Tziperman, 1992; Walin, 1982). The surface-forced overturning streamfunction (Ψ_s ; in units of Sv) across an isopycnal, σ , was calculated as (e.g., Marsh, 2000):

$$\Psi_s(\sigma^*) = \frac{1}{\Delta\sigma} \iint_{dA} \left[-\frac{\alpha Q_H}{C_p} + \beta \frac{S}{1-S} Q_{FW} \right] \Pi(\sigma) dA, \quad (1)$$

where

$$\Pi(\sigma) = \begin{cases} 1 & \text{if } \sigma - \Delta\sigma/2 < \sigma < \sigma + \Delta\sigma/2 \\ 0 & \text{elsewhere} \end{cases}$$

α is the thermal expansion coefficient, β is the haline contraction coefficient, C_p is the specific heat capacity of seawater, Q_H net surface heat flux into the ocean, S is surface salinity, and Q_{FW} is the net freshwater flux into the ocean that includes evaporation, precipitation, sea ice melting/freezing, and river runoff. Ψ_s was calculated for each month and each isopycnal σ (spaced by $\Delta\sigma = 0.1 \text{ kg m}^{-3}$) and then averaged into annual and regional fields. If σ did not outcrop within this region in a given month, Ψ_s was set to zero. Maps of Ψ_s were obtained by accumulating the integrand over outcrops (Desbruyères et al., 2019; Petit et al., 2020).

The surface-forced overturning in the Nordic Seas (Figure 1b) was calculated based on buoyancy fluxes and surface hydrography from ORAS5 (1979–2018) and its backward extension ORAS5-BE (1958–1978). For ORAS5, the ensemble spread provides an estimate of uncertainty for the monthly Ψ_s . In addition, we calculate Ψ_s based on surface heat fluxes (SHF) from the atmospheric reanalysis products ERA5 (1959–2020) (Hersbach et al., 2020), NOAA-20C (1900–2015) (Compo et al., 2011), and the Objectively Analyzed Air-Sea Fluxes for the Global Ocean (OAFlux, 1958–2020) (Yu et al., 2008). For OAFlux, only turbulent heat fluxes are available which leads to higher values of annual Ψ_s . When plotting Ψ_s from OAFlux, values are thus reduced by 1.5 Sv (based on sensitivity calculations from ORAS5 and NOAA-20C). Salinity is also not available for ERA5, NOAA-20C, and OAFlux and this was set to 35.2 (corresponding to AW salinities; Figure 2a). This is justified as surface density in the Atlantic domain of the Nordic Seas, which is the focus region of the calculations of Ψ_s based on atmospheric reanalysis data, is predominantly determined by temperature. Calculating Ψ_s with constant salinity in ORAS5 leads to minor changes (not shown). To accentuate multi-year variability a 2-year low-pass triangular filter (4-year filter width) was applied to the time series of surface-forced overturning and overflow transport.

The overturning streamfunction in density-space, Ψ_σ , across the GSR is calculated by summing the zonally-integrated transports from the densest levels to the lightest levels (e.g., Menary et al., 2020):

$$\Psi_\sigma = - \int_{x_w}^{x_e} \int_{\sigma_{\max}}^{\sigma_{\min}} v(x, \sigma) d\sigma dx \quad (2)$$

The overturning strength, defined as the maximum streamfunction, closely corresponds to the transport of overflow waters across the GSR (Figure S2 in Supporting Information S1).

3. Overflow Variability Determined by Surface Forcing in the Norwegian Sea

The mean streamfunction of the surface-forced Nordic Seas overturning circulation (Ψ_s) closely resembles the time-averaged overturning stream function in density space (Ψ_σ ; Figure 2b), supporting a clear link between the

Nordic Seas overturning and water mass transformation due to surface forcing. The surface-forced overturning reaches its maximum at $\sigma_\theta = 27.60 \text{ kg m}^{-3}$, which is slightly lighter than the density level of maximum overturning (27.75 kg m^{-3}). This suggests that additional transformation takes place that is not driven by surface buoyancy forcing, for example, through lateral exchange (mixing) between the boundary currents and the interior of the Nordic Seas (Evans et al., 2023; Huang et al., 2023; Isachsen et al., 2012).

As the aim of this study is to assess how variable surface-forced overturning manifests in the dense overflows across the GSR, we next compare the time series of Ψ_s at each density level with the time series of overflow transport. We find that Ψ_s at $\sigma_\theta = 27.50 \text{ kg m}^{-3}$ (hereafter referred to as $\Psi_s^{27.50}$) can account for a large fraction ($r = 0.81$) of the multi-annual overflow variability (Figures 3a and 3b). In contrast, overflow variability is not associated with Ψ_s at overflow densities ($>27.80 \text{ kg m}^{-3}$) or with the time series of maximum Ψ_s ($r = 0.08$ for detrended time series). The high correlation between $\Psi_s^{27.50}$ and total overflow transport across the GSR is reflected in both the DS and Iceland-Scotland overflow branch ($r = 0.83$ and $r = 0.53$, respectively).

There is no time lag between the surface-forced overturning and overflow transports, and higher correlations are not obtained if SHF are integrated over previous years. This is somewhat in contrast with findings of Tooth et al. (2023) who found that Nordic Seas overflow pathways integrate several decades of water mass transformation before crossing the GSR. However, a substantial part of the DS overflow is supplied by intermediate-depth Atlantic-origin overflow water (Harden et al., 2016; Håvik et al., 2019), which has a shorter residence time in the Nordic Seas and, hence, can contribute more directly to overflow variability (Eldevik et al., 2009). Considering the DS overflow separately, the overflow lags the surface-forced overturning by 1 year. No lag is found for the FSC, reflecting a shorter circulation loop within the Norwegian Sea (Chafik et al., 2020; Eldevik et al., 2009).

The concurrent relationship between $\Psi_s^{27.50}$ and overflow transport could be a result of large scale atmospheric forcing that can influence both water mass transformation in the Nordic Seas and the overflow across the GSR. Specifically, it is well documented that the North Atlantic Oscillation (NAO), the leading mode of sea level pressure variability in the North Atlantic, influences the exchanges across the GSR (e.g., Bringedal et al., 2018; Sandø et al., 2012). However, neither $\Psi_s^{27.50}$ nor the overflow transport is significantly correlated with the winter NAO index (p -value > 0.05). In line with observations (Bringedal et al., 2018), significant co-variability exists between the NAO and the overflow through the Faroe Bank Channel, but not with the total overflow transport which is analyzed here. A limited role of atmospheric forcing on total overflow variability is further supported by regressing the time series of overflow transport onto sea level pressure, showing a weak pattern with low correlations (Figure S3 in Supporting Information S1).

The spatial pattern of transformation across 27.50 kg m^{-3} (Figure 3c; calculated as described in Section 2.3) shows that water mass transformation into this density class predominantly occurs along the Atlantic water pathways in the eastern subpolar North Atlantic and Nordic Seas (Figure 1a). In the Nordic Seas, this corresponds to the Norwegian Atlantic Current (NwAC) and the West Spitsbergen Current flowing northwards along the coast of Norway and Svalbard, respectively. Integrating the water mass transformation over four different regions shows that 87% of $\Psi_s^{27.50}$ takes place in the Norwegian Sea (Figure 3d). Consistent with observations (Brakstad et al., 2023; Huang et al., 2020), the transformation into denser water masses shifts progressively toward the Fram Strait and Greenland Sea. These results imply that although the densest overflow waters are produced in the Greenland Sea, this is not the main source region for multi-annual variability in overflow waters across GSR.

Surface transformation of Atlantic waters also takes place in the Arctic Ocean, and especially in the Barents Sea (Årthun et al., 2011; Rudels et al., 1999). However, no significant correlations are found between the surface-forced overturning in the Arctic Ocean (bounded by the Fram Strait, Barents Sea Opening, and Bering Strait) and the overflow transport across the GSR (Figure S4 in Supporting Information S1). Including the Arctic Ocean in the calculation of surface-forced overturning does also not have a notable influence on $\Psi_s^{27.50}$ and its relationship to overflow. It also does not lead to any other density levels becoming significantly related to overflow transport.

4. Multidecadal Variability of the Surface-Forced Overturning Circulation

Motivated by the strong correlation between overflow variability and $\Psi_s^{27.50}$ we calculate the surface-forced overturning circulation over an extended time period using three different reanalyses products (ERA5, NOAA-20C and OAFlux; Methods), as well as the backward extension of ORAS5 (ORAS5-BE). The surface-forced

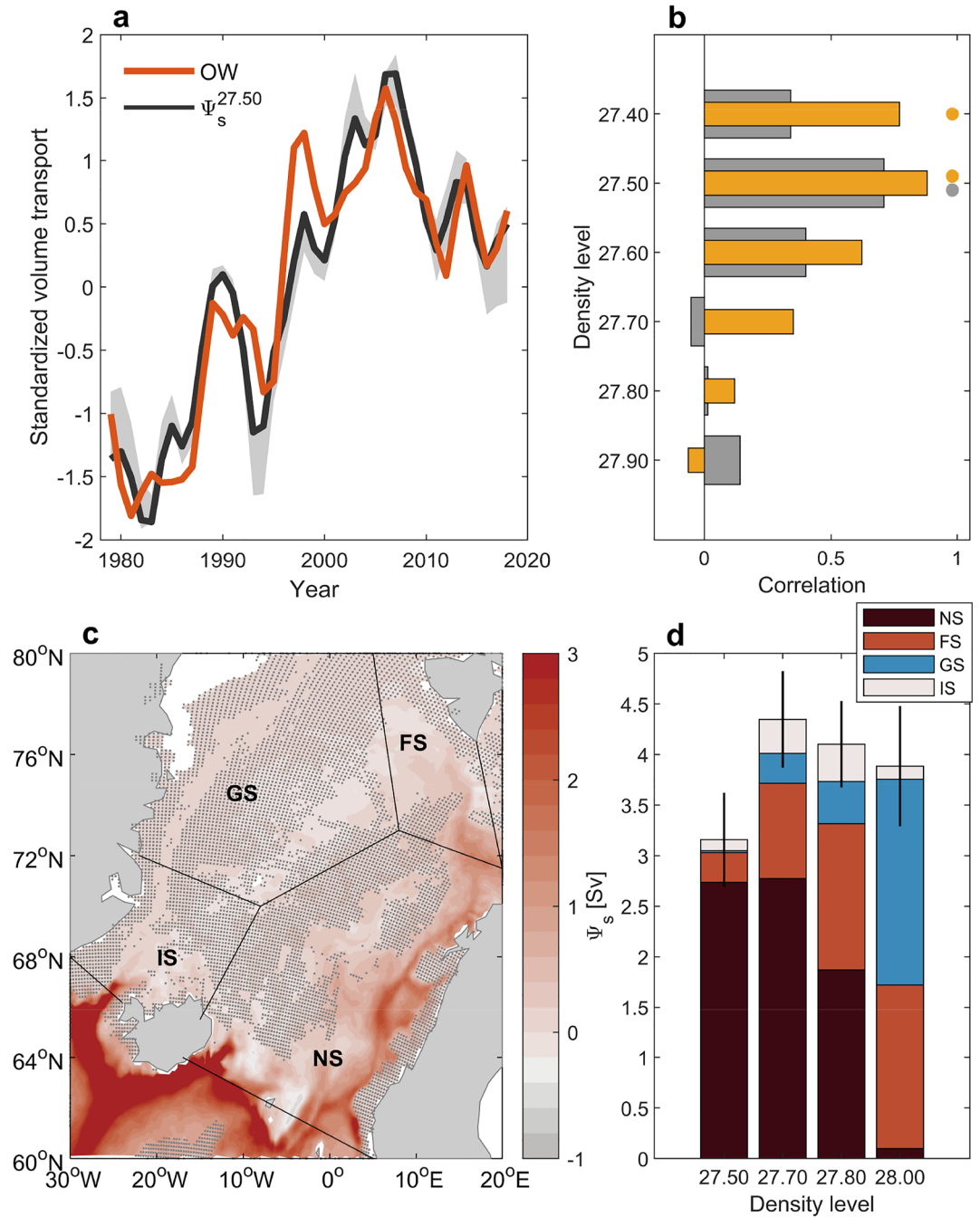


Figure 3. (a) Standardized time series of overflow transport (OW) and surface-forced overturning at $\sigma_\theta = 27.50 \text{ kg m}^{-3}$ ($\Psi_s^{27.50}$) in ORAS5. The gray shading is the ORAS5 ensemble spread for $\Psi_s^{27.50}$. Time series were standardized by removing the mean and dividing by the standard deviation. (b) Correlations between overflow transport and Ψ_s at different density levels. Gray (orange) bars show correlations for linearly detrended (full) data. Significant correlations at the 95% confidence level (Ebisuzaki, 1997) are indicated by filled circles. (c) Spatial pattern of mean surface-forced overturning at $\sigma_\theta = 27.50 \text{ kg m}^{-3}$ (units: 10^{-3} Sv) in ORAS5 between 1979 and 2018. Positive values correspond to densification to this isopycnal. Gray dots indicate where the isopycnal outcropped less than, on average, once per year. NS, Norwegian Sea; FS, Fram Strait; GS, Greenland Sea; IS, Iceland Sea. (d) The mean contribution to surface-forced overturning at different density levels by different regions. Vertical lines show standard deviation of the corresponding detrended time series.

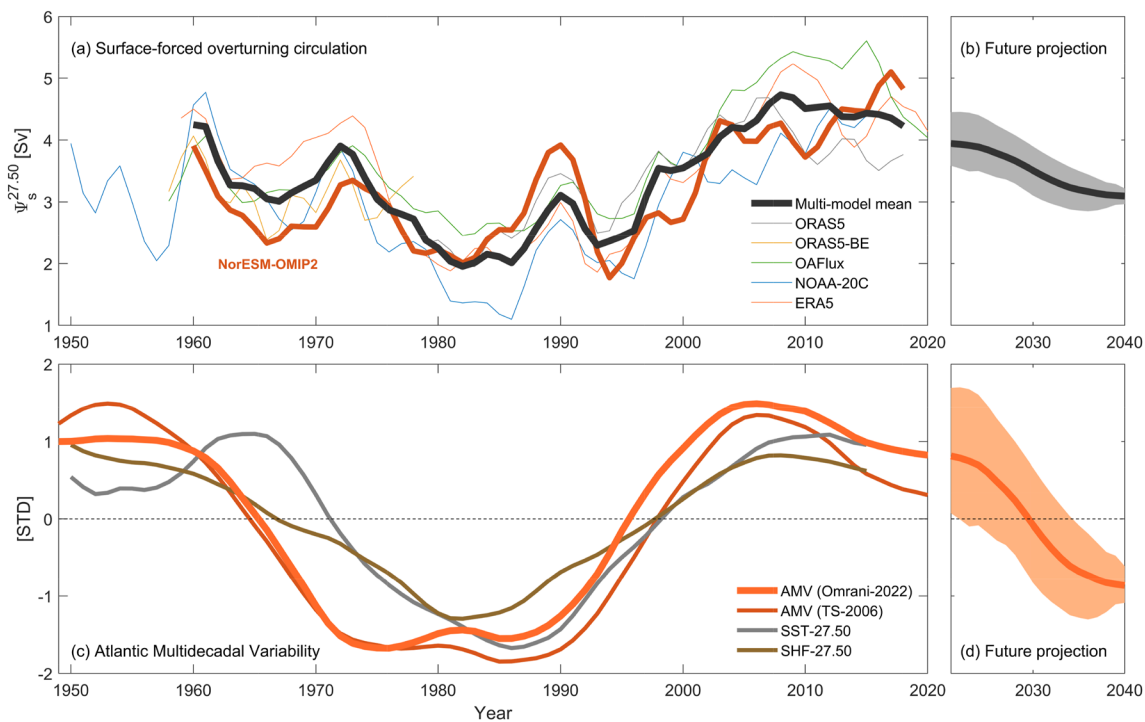


Figure 4. (a and b) Surface-forced overturning at $\sigma_{\theta} = 27.50 \text{ kg m}^{-3}$ in the Nordic Seas ($\Psi_s^{27.50}$) for different reanalysis products. Thick black line shows the multi-model mean for 1960–2018 when there is at least three products available. The thick red line shows $\Psi_s^{27.50}$ calculated from the NorESM OMIP2 simulation. (c and d) Multidecadal sea-surface temperature (SST) variability in the North Atlantic represented by the AMV-index (Omrani et al., 2022; Trenberth & Shea, 2006), and SST and surface heat fluxes (SHF) from NOAA-20C averaged over the surface area of $\Psi_s^{27.50}$. Time series have been linearly detrended, standardized and 10-year low-pass filtered to highlight multidecadal variability. Positive SHF indicates oceanic heat loss. Projections of Atlantic Multidecadal Variability in (d) are from Omrani et al. (2022) and are used to infer future $\Psi_s^{27.50}$ plotted in (b) through linear regression of the multi-model mean surface-forced overturning against the AMV-index between 1960 and 2018. Solid line is the ensemble mean and shading represents the interquartile range based on different statistical projections (see Omrani et al., 2022).

overturning at $\sigma_{\theta} = 27.50 \text{ kg m}^{-3}$ based on these reanalyses shows good agreement with ORAS5 for the recent decades (Figure 4a), providing confidence in the results. Considering the extended period since 1950, it is seen that the increased $\Psi_s^{27.50}$ after the 1980s was preceded by a notable decrease. These reconstructions thus suggest pronounced multidecadal variability in Nordic Seas surface-forced overturning circulation, and, hence, overflow transport. The temporal evolution of this multidecadal reconstruction of $\Psi_s^{27.50}$ is further supported by a simulation by the Norwegian Earth System Model (NorESM2-LM; Seland et al., 2020) forced by the Japanese atmospheric reanalysis product JRA55-do (Tsujino et al., 2018) as part of the Ocean Model Intercomparison Project Phase 2 (OMIP-2; Griffies et al., 2016).

Variations in surface-forced overturning can be driven by both air-sea fluxes and by the area covered by a particular surface density range (Equation 1). All the reanalyses considered here suggest that the surface area is most important to $\Psi_s^{27.50}$ ($r = 0.70 - 0.85$; Figure S5 in Supporting Information S1). The finding that the variance in Atlantic water transformation is mainly influenced by the variance in density at the ocean surface is in agreement with results from the subpolar North Atlantic (Petit et al., 2021).

The multidecadal signal in Nordic Seas surface-forced overturning circulation closely resembles that found in North Atlantic sea-surface temperatures, that is, the Atlantic Multidecadal Variability (AMV; Trenberth & Shea, 2006) (Figure 4c). Similar variations of Iceland-Scotland overflow strength and the AMV in palaeo-reconstructions and preindustrial control simulations were also noted by Lohmann et al. (2015). In agreement with our results, they argued that the similar variation of Iceland-Scotland overflow strength and AMV index is due to changes in the density structure of the Nordic Seas, which is positively correlated with the AMV index. However, whereas we find surface density to influence overflow transport by affecting the transformation of surface water, Lohmann et al. (2015) found AMV-related surface density changes to affect the pressure gradient, and, hence, the transport across the GSR.

Following Olsen et al. (2008) and Bringedal et al. (2018), we calculate the pressure gradient across the GSR using the difference in sea-surface height (barotropic component) and density at 700-m depth (baroclinic component) between an area north (64–66°N, 0–4°W) and south (60–61°N, 16–18°W) of the ridge. Consistent with observations (Bringedal et al., 2018), the relation between overflow transport and pressure differences is mainly determined by the barotropic component ($r = 0.55$). The baroclinic pressure difference ($r = 0.31$) still contributes to the total pressure gradient ($r = 0.71$), but predominantly as a result of density changes south of the GSR. The co-variability between $\Psi_s^{27.50}$ and overflow transport across GSR can therefore not be ascribed to density changes in the Nordic Seas driving both $\Psi_s^{27.50}$ and baroclinic transports.

A quantitative analysis of the mechanisms driving variable surface hydrography in the Nordic Seas, and how this is related to the AMV, is not preformed here. Previous studies have, however, shown that anomalous advection of Atlantic Water into the Nordic Seas plays a key role (Årthun et al., 2017; Asbjørnsen et al., 2019; Carton et al., 2011). A dominant role of ocean advection in driving surface density changes is furthermore supported by higher sea-surface temperatures being associated with anomalous heat fluxes out of the ocean (Figure 4c; shown for NOAA-20C but also true for ORAS5 and OAFux). A connection between the Nordic Seas and the North Atlantic is further supported by recent reconstructions of the Atlantic inflow across the GSR (Rossby et al., 2020) that also shows clear multidecadal variability.

The finding that the overturning circulation in the Nordic Seas displays pronounced multidecadal variability in connection with hydrographic variations in the upper ocean is in line with some observation-based reconstructions of the overturning circulation in the subpolar North Atlantic (Fraser & Cunningham, 2021; Jackson et al., 2022). Other estimates, however, find that the North Atlantic overturning strength shows no clear connectivity to upper-ocean density changes and no distinct decadal to multidecadal variability (Fu et al., 2020). Uncertainty thus remains about multidecadal trends in the North Atlantic overturning circulation and to what extent these are influenced by long-term variations in Nordic Seas overturning and overflow waters (Figure 4a).

Observation-based projections of the AMV suggest that it is currently transitioning into its negative phase (Frajka-Williams et al., 2017; Omrani et al., 2022) (Figures 4c and 4d). Considering the identified link between the AMV and Nordic Seas overturning circulation, this implies the next decades could see a decreased overturning circulation in the Nordic Seas. Based on the linear sensitivity of the 10-year low-pass filtered $\Psi_s^{27.50}$ to changes in the AMV (averaged over the different data sets), the AMV-decline toward 2040 corresponds to a 0.8 Sv reduction in overturning circulation (Figure 4b). A reduced Nordic Seas overturning circulation toward 2040 of similar magnitude is also seen in climate model simulations, followed by a subsequent strengthening toward the end of the century (Årthun et al., 2023). It is important to keep in mind, however, that other processes will also affect the future strength of the Nordic Seas overturning circulation. For example, ongoing sea ice loss in the Greenland Sea can lead to enhanced ventilation of the Atlantic water boundary current (Moore et al., 2022; Våge et al., 2018), which would act to increase overturning in this region.

5. Conclusions and Implications

In this study, we have used ocean and atmospheric reanalyses to assess the role of surface-forced water mass transformation (overturning) in Nordic Seas overflow variability. We find that a majority of overflow variability is determined by transformation of Atlantic water along the NwAC ($\Psi_s^{27.50}$; Figure 3). The production of dense water masses in the Greenland and Iceland Seas is of minor importance to overflow variability. Our results thus support a direct export pathway of modified Atlantic water, that is, Atlantic-origin overflow water, as the main source of overflow water variability (Eldevik et al., 2009; Mauritzen, 1996). The finding that surface-forced water mass transformation of a specific density level can explain a large fraction of overflow variability has potential implications for monitoring of the overflows. Overflows are notoriously hard to observe from current meters, but results presented here imply that Nordic Seas overturning and associated overflow transport may be diagnosed by observing processes at the sea surface.

Because of its role in feeding the lower limb of the AMOC, the potential of a weakened Nordic Seas overflow transport is of great interest and concern (Hansen et al., 2001; Köhl et al., 2007; Olsen et al., 2008; Zhang et al., 2004; Østerhus et al., 2019). Here we show, using different reanalyses products, that the transformation of Atlantic water into overflow waters shows no long-term trend, but is rather characterized by pronounced multidecadal variability in synchrony with the AMV. The presence of multidecadal variability in the water mass

transformation in the Nordic Seas and transport across GSR needs to be taken into account when interpreting observations that only cover a limited time period (e.g., Hansen et al., 2001; Tsubouchi et al., 2021). As the AMV is currently transitioning into its negative phase (Omrani et al., 2022), the next decades could see a decreased overflow from the Nordic Seas.

Data Availability Statement

All the data used in this study are publicly available. ORAS5 data are available from <https://doi.org/10.24381/cds.67e8eeb7> (Zuo et al., 2019); ERA5 from ECMWF <https://doi.org/10.24381/cds.f17050d7> (Hersbach et al., 2020); NOAA-20C from https://psl.noaa.gov/data/gridded/data.20thC_ReanV3.html (Compo et al., 2011); OAFflux from Woods Hole Oceanographic Institution <https://oafux.whoi.edu/data-access/> (Yu et al., 2008). Data from C-GLORSv7, GLORYS2V4, and GloSea5 are available from Copernicus Marine Service (CMS, 2022) <https://doi.org/10.48670/moi-00023>. OMIP2 output from NorESM2 were obtained from <https://esgf-data.dkrz.de/projects/esgf-dkrz/>. Observed transports across the GSR are from AtlantOS (OceanSITES, 2022) <http://www.oceansites.org/tma/gsr.html> and the AMV index from NCAR Climate Data Guide (NCAR CDG, 2022) <https://climatedataguide.ucar.edu/climate-data/atlantic-multi-decadal-oscillation-amv>.

Acknowledgments

This study has received funding from the Trond Mohn Foundation (project number BFS2018TMT01bcpu) and the Bjerknes Centre for Climate Research (strategic project DYNASOR). The author thanks two anonymous reviewers for valuable comments that improved the manuscript, Nour-Eddine Omrani for providing the AMV projections in Figure 4d, and Kjetil Våge, Tor Eldevik, and Helene Asbjørnsen for fruitful discussions.

References

- Årthun, M., Asbjørnsen, H., Chafik, L., Johnson, H., & Våge, K. (2023). Future strengthening of the Nordic Seas overturning circulation. *Nature Communications*, 14(1), 2065. <https://doi.org/10.1038/s41467-023-37846-6>
- Årthun, M., Eldevik, T., Viste, E., Drange, H., Furevik, T., Johnson, H. L., & Keenlyside, N. S. (2017). Skillful prediction of northern climate provided by the ocean. *Nature Communications*, 8(1), 15875. <https://doi.org/10.1038/ncomms15875>
- Årthun, M., Ingvaldsen, R., Smedsrud, L. H., & Schrum, C. (2011). Dense water formation and circulation in the Barents Sea. *Deep-Sea Research*, 58(8), 801–817. <https://doi.org/10.1016/j.dsr.2011.06.001>
- Asbjørnsen, H., Årthun, M., Skagseth, Ø., & Eldevik, T. (2019). Mechanisms of ocean heat anomalies in the Norwegian Sea. *Journal of Geophysical Research: Oceans*, 124(4), 2908–2923. <https://doi.org/10.1029/2018jc014649>
- Brakstad, A., Gebbie, G., Våge, K., Jeansson, E., & Ólafsdóttir, S. R. (2023). Formation and pathways of dense water in the Nordic Seas based on a regional inversion. *Progress in Oceanography*, 212, 102981. <https://doi.org/10.1016/j.pocan.2023.102981>
- Brakstad, A., Våge, K., Håvik, L., & Moore, G. (2019). Water mass transformation in the Greenland Sea during the period 1986–2016. *Journal of Physical Oceanography*, 49(1), 121–140. <https://doi.org/10.1175/jpo-d-17-0273.1>
- Bringedal, C., Eldevik, T., Skagseth, Ø., Spall, M. A., & Østerhus, S. (2018). Structure and forcing of observed exchanges across the Greenland–Scotland Ridge. *Journal of Climate*, 31(24), 9881–9901. <https://doi.org/10.1175/jcli-d-17-0889.1>
- Carton, J. A., Chepurin, G. A., Reagan, J., & Häkkinen, S. (2011). Interannual to decadal variability of Atlantic Water in the Nordic and adjacent seas. *Journal of Geophysical Research*, 116(C11), C11035. <https://doi.org/10.1029/2011jc007102>
- Carton, J. A., Penny, S. G., & Kalnay, E. (2019). Temperature and salinity variability in the SODA3, ECCO4r3, and ORAS5 ocean reanalyses, 1993–2015. *Journal of Climate*, 32(8), 2277–2293. <https://doi.org/10.1175/jcli-d-18-0605.1>
- Chafik, L., Hátún, H., Kjellsson, J., Larsen, K. M. H., Rossby, T., & Børja, B. (2020). Discovery of an unrecognized pathway carrying overflow waters toward the Faroe Bank Channel. *Nature Communications*, 11(1), 3721. <https://doi.org/10.1038/s41467-020-17426-8>
- Chafik, L., & Rossby, T. (2019). Volume, heat, and freshwater divergences in the subpolar North Atlantic suggest the Nordic Seas as key to the state of the meridional overturning circulation. *Geophysical Research Letters*, 46(9), 4799–4808. <https://doi.org/10.1029/2019gl082110>
- CMS. (2022). Global Ocean Ensemble Physics Reanalysis - Low resolution [Dataset]. Copernicus Marine Service. <https://doi.org/10.48670/moi-00023>
- Compo, G. P., Whitaker, J. S., Sardeshmukh, P. D., Matsui, N., Allan, R. J., Yin, X., et al. (2011). The twentieth century reanalysis project. *Quarterly Journal of the Royal Meteorological Society*, 137(654), 1–28. <https://doi.org/10.1002/qj.776>
- Desbryères, D. G., Mercier, H., Maze, G., & Danialt, N. (2019). Surface predictor of overturning circulation and heat content change in the subpolar North Atlantic. *Ocean Science*, 15(3), 809–817. <https://doi.org/10.5194/os-15-809-2019>
- Dickson, R. R., & Brown, J. (1994). The production of North Atlantic Deep Water: Sources, rates, and pathways. *Journal of Geophysical Research*, 99(C6), 12319–12341. <https://doi.org/10.1029/94jc00530>
- Ebisuzaki, W. (1997). A method to estimate the statistical significance of a correlation when the data are serially correlated. *Journal of Climate*, 10(9), 2147–2153. [https://doi.org/10.1175/1520-0442\(1997\)010<2147:amets>2.0.co;2](https://doi.org/10.1175/1520-0442(1997)010<2147:amets>2.0.co;2)
- Eldevik, T., & Nilsen, J. E. Ø. (2013). The Arctic–Atlantic thermohaline circulation. *Journal of Climate*, 26(21), 8698–8705. <https://doi.org/10.1175/jcli-d-13-00305.1>
- Eldevik, T., Nilsen, J. E. Ø., Iovino, D., Olsson, K. A., Sandø, A. B., & Drange, H. (2009). Observed sources and variability of Nordic seas overflow. *Nature Geoscience*, 2(6), 406–410. <https://doi.org/10.1038/ngeo518>
- Evans, D. G., Holliday, N. P., Bacon, S., & Le Bras, I. (2023). Mixing and air–sea buoyancy fluxes set the time-mean overturning circulation in the subpolar North Atlantic and Nordic Seas. *Ocean Science*, 19(3), 745–768. <https://doi.org/10.5194/os-19-745-2023>
- Ferry, N., Parent, L., Garric, G., Bricaud, C., Testut, C., Le Galloudec, O., et al. (2012). GLORYS2V1 global ocean reanalysis of the altimetric era (1992–2009) at mesoscale. *Mercator Ocean–Quarterly Newsletter*, 44, 29–39.
- Frajka-Williams, E., Beaulieu, C., & Duche, A. (2017). Emerging negative Atlantic Multidecadal Oscillation index in spite of warm subtropics. *Scientific Reports*, 7(1), 1–8. <https://doi.org/10.1038/s41598-017-11046-x>
- Fraser, N. J., & Cunningham, S. A. (2021). 120 Years of AMOC variability reconstructed from observations using the Bernoulli inverse. *Geophysical Research Letters*, 48(18), e2021GL093893. <https://doi.org/10.1029/2021gl093893>
- Fu, Y., Li, F., Karstensen, J., & Wang, C. (2020). A stable Atlantic meridional overturning circulation in a changing North Atlantic Ocean since the 1990s. *Science Advances*, 6(48), eabc7836. <https://doi.org/10.1126/sciadv.abc7836>

- Griffies, S. M., Danabasoglu, G., Durack, P. J., Adcroft, A. J., Balaji, V., Böning, C. W., et al. (2016). OMIP contribution to CMIP6: Experimental and diagnostic protocol for the physical component of the Ocean Model Intercomparison Project. *Geoscientific Model Development*, 9, 3231–3296. <https://doi.org/10.5194/gmd-9-3231-2016>
- Hansen, B., Larsen, K. M., Hátún, H., & Østerhus, S. (2016). A stable Faroe Bank Channel overflow 1995–2015. *Ocean Science*, 12(6), 1205–1220. <https://doi.org/10.5194/os-12-1205-2016>
- Hansen, B., & Østerhus, S. (2000). North Atlantic–Nordic Seas exchanges. *Progress in Oceanography*, 45(2), 109–208. [https://doi.org/10.1016/S0079-6611\(99\)00052-X](https://doi.org/10.1016/S0079-6611(99)00052-X)
- Hansen, B., Turrell, W. R., & Østerhus, S. (2001). Decreasing overflow from the Nordic seas into the Atlantic Ocean through the Faroe Bank channel since 1950. *Nature*, 411(6840), 927–930. <https://doi.org/10.1038/35082034>
- Harden, B. E., Pickart, R. S., Valdimarsson, H., Våge, K., de Steur, L., Richards, C., et al. (2016). Upstream sources of the Denmark Strait Overflow: Observations from a high-resolution mooring array. *Deep Sea Research Part I: Oceanographic Research Papers*, 112, 94–112. <https://doi.org/10.1016/j.dsr.2016.02.007>
- Håvik, L., Almansí, M., Våge, K., & Haine, T. W. (2019). Atlantic-origin overflow water in the East Greenland Current. *Journal of Physical Oceanography*, 49(9), 2255–2269. <https://doi.org/10.1175/jpo-d-18-0216.1>
- Hersbach, H., Bell, B., Berrisford, P., Hirahara, S., Horányi, A., Muñoz-Sabater, J., et al. (2020). The ERA5 global reanalysis. *Quarterly Journal of the Royal Meteorological Society*, 146(730), 1999–2049. <https://doi.org/10.1002/qj.3803>
- Huang, J., Pickart, R. S., Chen, Z., & Huang, R. X. (2023). Role of air-sea heat flux on the transformation of Atlantic Water encircling the Nordic Seas. *Nature Communications*, 14(1), 141. <https://doi.org/10.1038/s41467-023-35889-3>
- Huang, J., Pickart, R. S., Huang, R. X., Lin, P., Brakstad, A., & Xu, F. (2020). Sources and upstream pathways of the densest overflow water in the Nordic Seas. *Nature Communications*, 11(1), 1–9. <https://doi.org/10.1038/s41467-020-19050-y>
- Isachsen, P., Koszalka, I., & LaCasce, J. (2012). Observed and modeled surface eddy heat fluxes in the eastern Nordic Seas. *Journal of Geophysical Research*, 117(C8), C08020. <https://doi.org/10.1029/2012jc007935>
- Isachsen, P., Mauritzen, C., & Svendsen, H. (2007). Dense water formation in the Nordic Seas diagnosed from sea surface buoyancy fluxes. *Deep Sea Research Part I: Oceanographic Research Papers*, 54(1), 22–41. <https://doi.org/10.1016/j.dsr.2006.09.008>
- Jackson, L. C., Biastoch, A., Buckley, M. W., Desbruyères, D. G., Frajka-Williams, E., Moat, B., & Robson, J. (2022). The evolution of the North Atlantic Meridional Overturning Circulation since 1980. *Nature Reviews Earth & Environment*, 3(4), 1–14. <https://doi.org/10.1038/s43017-022-00263-2>
- Jochumsen, K., Moritz, M., Nunes, N., Quadfasel, D., Larsen, K. M., Hansen, B., et al. (2017). Revised transport estimates of the Denmark Strait overflow. *Journal of Geophysical Research: Oceans*, 122(4), 3434–3450. <https://doi.org/10.1002/2017jc012803>
- Köhl, A., Käse, R. H., Stammer, D., & Serra, N. (2007). Causes of changes in the Denmark Strait overflow. *Journal of Physical Oceanography*, 37(6), 1678–1696. <https://doi.org/10.1175/jpo3080.1>
- Li, Z., Ding, Q., Steele, M., & Schweiger, A. (2022). Recent upper Arctic Ocean warming expedited by summertime atmospheric processes. *Nature Communications*, 13(1), 1–11. <https://doi.org/10.1038/s41467-022-28047-8>
- Lohmann, K., Mignot, J., Langehaug, H. R., Jungclauss, J. H., Matei, D., Otterå, O. H., et al. (2015). Using simulations of the last millennium to understand climate variability seen in palaeo-observations: Similar variation of Iceland–Scotland overflow strength and Atlantic Multidecadal Oscillation. *Climate of the Past*, 11(2), 203–216. <https://doi.org/10.5194/cp-11-203-2015>
- MacLachlan, C., Arribas, A., Peterson, K. A., Maidens, A., Fereday, D., Scaife, A., et al. (2015). Global Seasonal forecast system version 5 (GloSea5): A high-resolution seasonal forecast system. *Quarterly Journal of the Royal Meteorological Society*, 141(689), 1072–1084. <https://doi.org/10.1002/qj.2396>
- Marsh, R. (2000). Recent variability of the North Atlantic thermohaline circulation inferred from surface heat and freshwater fluxes. *Journal of Climate*, 13(18), 3239–3260. [https://doi.org/10.1175/1520-0442\(2000\)013<3239:rivotna>2.0.co;2](https://doi.org/10.1175/1520-0442(2000)013<3239:rivotna>2.0.co;2)
- Mauritzen, C. (1996). Production of dense overflow waters feeding the North Atlantic across the Greenland–Scotland Ridge. Part 1: Evidence for a revised circulation scheme. *Deep Sea Research Part I: Oceanographic Research Papers*, 43(6), 769–806. [https://doi.org/10.1016/0967-0637\(96\)00037-4](https://doi.org/10.1016/0967-0637(96)00037-4)
- Megann, A., Blaker, A., Josey, S., New, A., & Sinha, B. (2021). Mechanisms for late 20th and early 21st century decadal AMOC variability. *Journal of Geophysical Research: Oceans*, 126(12), e2021JC017865. <https://doi.org/10.1029/2021jc017865>
- Menary, M. B., Jackson, L. C., & Lozier, M. S. (2020). Reconciling the relationship between the AMOC and Labrador Sea in OSNAP observations and climate models. *Geophysical Research Letters*, 47(18), e2020GL089793. <https://doi.org/10.1029/2020gl089793>
- Moore, G., Våge, K., Renfrew, I., & Pickart, R. (2022). Sea-ice retreat suggests re-organization of water mass transformation in the Nordic and Barents Seas. *Nature Communications*, 13(1), 1–8. <https://doi.org/10.1038/s41467-021-27641-6>
- NCAR CDG. (2022). Atlantic Multi-decadal Oscillation (AMO) [Dataset]. NCAR Climate Data Guide. Retrieved from <https://climatedataguide.ucar.edu/climate-data/atlantic-multi-decadal-oscillation-amo>
- OceanSITES. (2022). Optimising and Enhancing the Integrated Atlantic Ocean Observing Systems, AtlantOS [Dataset]. AtlantOS project. Retrieved from <http://www.oceansites.org/tma/index.html>
- Olsen, S. M., Hansen, B., Quadfasel, D., & Østerhus, S. (2008). Observed and modelled stability of overflow across the Greenland–Scotland ridge. *Nature*, 455(7212), 519–522. <https://doi.org/10.1038/nature07302>
- Omrani, N.-E., Keenlyside, N., Matthes, K., Boljka, L., Zanchettin, D., Jungclauss, J. H., & Lubis, S. W. (2022). Coupled stratosphere-troposphere–Atlantic multidecadal oscillation and its importance for near-future climate projection. *npj Climate and Atmospheric Science*, 5(1), 1–14. <https://doi.org/10.1038/s41612-022-00275-1>
- Orvik, K. A., & Niiler, P. (2002). Major pathways of Atlantic water in the northern North Atlantic and Nordic Seas toward Arctic. *Geophysical Research Letters*, 29(19), 2–1. <https://doi.org/10.1029/2002gl015002>
- Østerhus, S., Woodgate, R., Valdimarsson, H., Turrell, B., De Steur, L., Quadfasel, D., et al. (2019). Arctic Mediterranean exchanges: A consistent volume budget and trends in transports from two decades of observations. *Ocean Science*, 15(2), 379–399. <https://doi.org/10.5194/os-15-379-2019>
- Petit, T., Lozier, M. S., Josey, S. A., & Cunningham, S. A. (2020). Atlantic deep water formation occurs primarily in the Iceland Basin and Irminger Sea by local buoyancy forcing. *Geophysical Research Letters*, 47(22), e2020GL091028. <https://doi.org/10.1029/2020gl091028>
- Petit, T., Lozier, M. S., Josey, S. A., & Cunningham, S. A. (2021). Role of air–sea fluxes and ocean surface density in the production of deep waters in the eastern subpolar gyre of the North Atlantic. *Ocean Science*, 17(5), 1353–1365. <https://doi.org/10.5194/os-17-1353-2021>
- Rosby, T., Chafik, L., & Houpert, L. (2020). What can hydrography tell us about the strength of the Nordic Seas MOC over the last 70 to 100 years? *Geophysical Research Letters*, 47(12), e2020GL087456. <https://doi.org/10.1029/2020gl087456>
- Rudels, B., Friedrich, H. J., & Quadfasel, D. (1999). The Arctic circumpolar boundary current. *Deep Sea Research Part II: Topical Studies in Oceanography*, 46(6–7), 1023–1062. [https://doi.org/10.1016/S0967-0645\(99\)00015-6](https://doi.org/10.1016/S0967-0645(99)00015-6)

- Sandø, A., Nilsen, J. Ø., Eldevik, T., & Bentsen, M. (2012). Mechanisms for variable North Atlantic–Nordic seas exchanges. *Journal of Geophysical Research*, *117*(C12), C12006. <https://doi.org/10.1029/2012jc008177>
- Seland, Ø., Bentsen, M., Olivie, D., Toniazzo, T., Gjermundsen, A., Graff, L. S., et al. (2020). Overview of the Norwegian Earth System Model (NorESM2) and key climate response of CMIP6 DECK, historical, and scenario simulations. *Geoscientific Model Development*, *13*(12), 6165–6200. <https://doi.org/10.5194/gmd-13-6165-2020>
- Shu, Q., Wang, Q., Song, Z., & Qiao, F. (2021). The poleward enhanced Arctic Ocean cooling machine in a warming climate. *Nature Communications*, *12*(1), 1–9. <https://doi.org/10.1038/s41467-021-23321-7>
- Smedsrud, L. H., Muilwijk, M., Brakstad, A., Madonna, E., Lauvset, S. K., Spensberger, C., et al. (2022). Nordic Seas heat loss, Atlantic inflow, and Arctic sea ice cover over the last century. *Reviews of Geophysics*, *60*(1), e2020RG000725. <https://doi.org/10.1029/2020rg000725>
- Speer, K., & Tziperman, E. (1992). Rates of water mass formation in the North Atlantic Ocean. *Journal of Physical Oceanography*, *22*(1), 93–104. [https://doi.org/10.1175/1520-0485\(1992\)022<0093:rowmfi>2.0.co;2](https://doi.org/10.1175/1520-0485(1992)022<0093:rowmfi>2.0.co;2)
- Storto, A., & Masina, S. (2016). C-GLORSv5: An improved multipurpose global ocean eddy-permitting physical reanalysis. *Earth System Science Data*, *8*(2), 679–696. <https://doi.org/10.5194/essd-8-679-2016>
- Swift, J. H., & Aagaard, K. (1981). Seasonal transitions and water mass formation in the Iceland and Greenland seas. *Deep Sea Research Part A. Oceanographic Research Papers*, *28*(10), 1107–1129. [https://doi.org/10.1016/0198-0149\(81\)90050-9](https://doi.org/10.1016/0198-0149(81)90050-9)
- Swift, J. H., Aagaard, K., & Malmberg, S.-A. (1980). The contribution of the Denmark Strait overflow to the deep North Atlantic. *Deep Sea Research Part A. Oceanographic Research Papers*, *27*(1), 29–42. [https://doi.org/10.1016/0198-0149\(80\)90070-9](https://doi.org/10.1016/0198-0149(80)90070-9)
- Tooth, O. J., Johnson, H. L., & Wilson, C. (2023). Lagrangian overturning pathways in the eastern Subpolar North Atlantic. *Journal of Climate*, *36*(3), 823–844. <https://doi.org/10.1175/jcli-d-21-0985.1>
- Trenberth, K. E., & Shea, D. J. (2006). Atlantic hurricanes and natural variability in 2005. *Geophysical Research Letters*, *33*(12), L12704. <https://doi.org/10.1029/2006gl026894>
- Tsubouchi, T., Våge, K., Hansen, B., Larsen, K. M. H., Østerhus, S., Johnson, C., et al. (2021). Increased ocean heat transport into the Nordic Seas and Arctic Ocean over the period 1993–2016. *Nature Climate Change*, *11*(1), 21–26. <https://doi.org/10.1038/s41558-020-00941-3>
- Tsujino, H., Urakawa, S., Nakano, H., Small, R. J., Kim, W. M., Yeager, S. G., et al. (2018). JRA-55 based surface dataset for driving ocean–sea-ice models (JRA55-do). *Ocean Modelling*, *130*, 79–139. <https://doi.org/10.1016/j.ocemod.2018.07.002>
- Våge, K., Papritz, L., Håvik, L., Spall, M. A., & Moore, G. W. K. (2018). Ocean convection linked to the recent ice edge retreat along east Greenland. *Nature Communications*, *9*(1), 1–8. <https://doi.org/10.1038/s41467-018-03468-6>
- Våge, K., Pickart, R. S., Spall, M. A., Valdimarsson, H., Jónsson, S., Torres, D. J., et al. (2011). Significant role of the North Icelandic Jet in the formation of Denmark Strait overflow water. *Nature Geoscience*, *4*(10), 723–727. <https://doi.org/10.1038/ngeo1234>
- Walín, G. (1982). On the relation between sea-surface heat flow and thermal circulation in the ocean. *Tellus*, *34*(2), 187–195. <https://doi.org/10.3402/tellusa.v34i2.10801>
- Yu, L., Jin, X., & Weller, R. A. (2008). *Multidecade global flux datasets from the objectively analyzed air-sea fluxes (OAFux) project: Latent and sensible heat fluxes, ocean evaporation, and related surface meteorological variables (Technical Report)*. Woods Hole Oceanographic Institution.
- Zhang, J., Steele, M., Rothrock, D. A., & Lindsay, R. W. (2004). Increasing exchanges at Greenland-Scotland Ridge and their links with the North Atlantic Oscillation and Arctic sea ice. *Geophysical Research Letters*, *31*(9), L09307. <https://doi.org/10.1029/2003gl019304>
- Zuo, H., Balmaseda, M. A., Tietsche, S., Mogensen, K., & Mayer, M. (2019). The ECMWF operational ensemble reanalysis–analysis system for ocean and sea ice: A description of the system and assessment. *Ocean Science*, *15*(3), 779–808. <https://doi.org/10.5194/os-15-779-2019>